Volume 13
Number 10
14 March 2021
Pages 1207–1310

Analytical Methods

rsc.li/methods

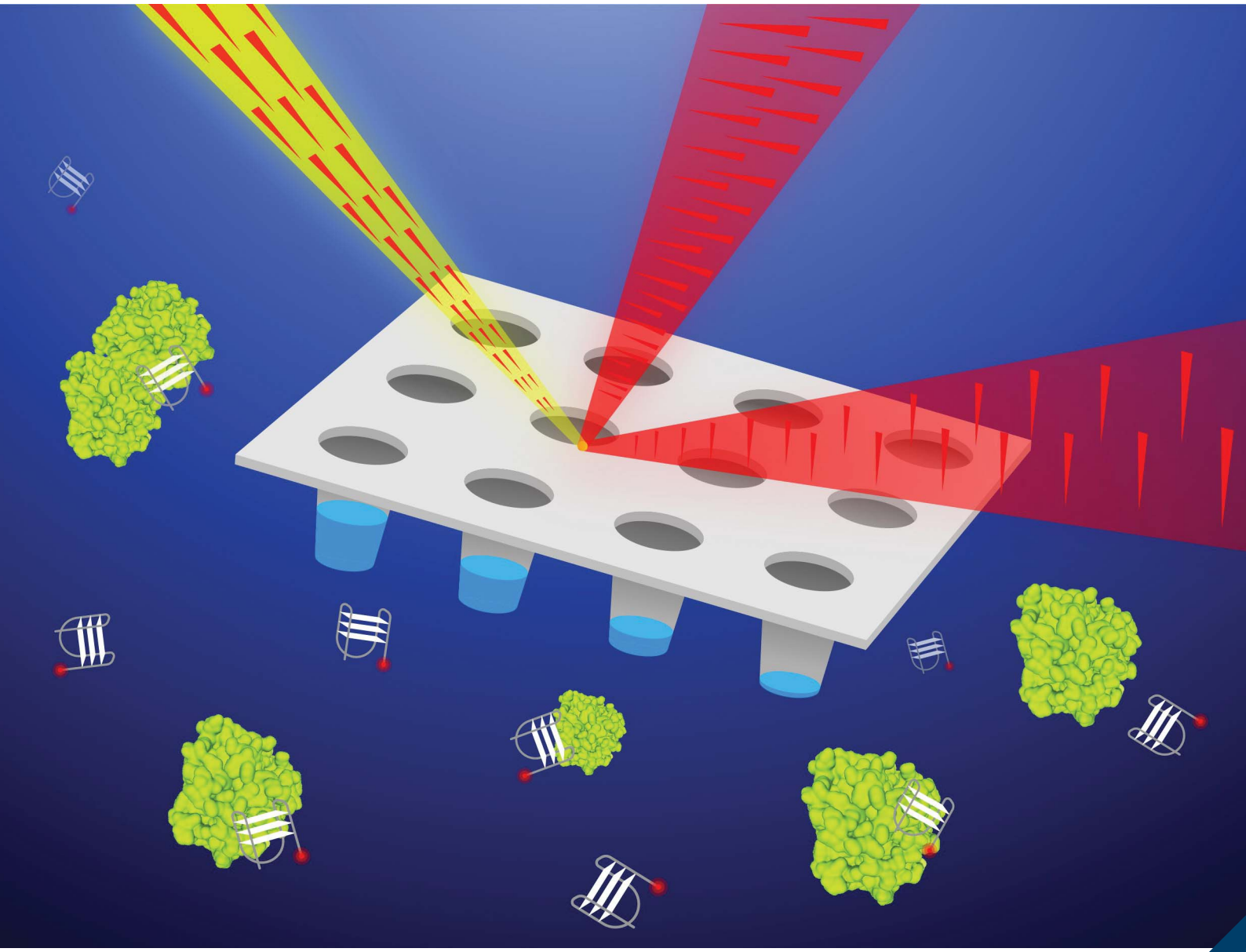

ISSN 1759-9679

ROYAL SOCIETY OF CHEMISTRY

TECHNICAL NOTE

Simon D. Weaver and Rebecca J. Whelan
Characterization of DNA aptamer–protein binding using fluorescence anisotropy assays in low-volume, high-efficiency plates

Analytical Methods

ROYAL SOCIETY OF CHEMISTRY

TECHNICAL NOTE

Cite this: *Anal. Methods*, 2021, **13**, 1302

Characterization of DNA aptamer–protein binding using fluorescence anisotropy assays in low-volume, high-efficiency plates†

Simon D. Weaver [a] and Rebecca J. Whelan *[b]

Received 10th December 2020
Accepted 27th January 2021

DOI: 10.1039/d0ay02256j

rsc.li/methods

Aptamers have many useful attributes including specific binding to molecular targets. After aptamers are identified, their target binding must be characterized. Fluorescence anisotropy (FA) is one technique that can be used to characterize affinity and to optimize aptamer–target interactions. Efforts to make FA assays more efficient by reducing assay volume and time from mixing to measurement may save time and resources by minimizing consumption of costly reagents. Here, we use thrombin and two thrombin-binding aptamers as a model system to show that plate-based FA experiments can be performed in volumes as low as 2 μL per well with 20 minute incubations with minimal loss in assay precision. We demonstrate that the aptamer–thrombin interaction is best modelled with the Hill equation, indicating cooperative binding. The miniaturization of this assay has implications in drug development, as well as in the efficiency of aptamer selection workflows by allowing for higher throughput aptamer analysis.

Introduction

Aptamers are short oligonucleotides with known sequence and one or more functional properties, which can include binding, cleavage, catalysis, and structure-switching.[1–3] Originally identified as RNA ligands that possessed the ability to bind organic dyes[4] or DNA polymerase,[5] these functional oligonucleotides now include natural single-stranded (ss) DNA[6] as well as modified RNA and DNA.[7,8] The targets of aptamers, meanwhile, span size and complexity scales ranging from small organic molecules,[9,10] through proteins[11,12] to cells.[13–15]

To the measurement scientist, the most compelling attribute of aptamers is their ability to function as a tool for molecular recognition complementary to antibodies.[16] Aptamers have been used as ligands in affinity-based separations;[17] to capture analytes onto surfaces prior to MALDI-mass spectrometry;[18] and in biosensors based on fluorometric,[19,20] colorimetric,[21,22] and electronic[23,24] signal transduction, among many other detection modalities.[25] Their sequence information can be shared as a simple text string, enabling any researcher to produce an identical reagent, unlike monoclonal and polyclonal antibodies, for which no analogous universal transfer is possible. Aptamers are most often identified through an *in vitro* evolution process called SELEX (Systematic Evolution of Ligands by EXponential enrichment),[5] that converges a large randomized population of input candidate molecules to a much smaller population of functional oligonucleotides. Alternative methods of aptamer selection have also been reported.[26,27]

At the conclusion of every aptamer selection process, it is necessary (at a minimum) to determine the stoichiometry and binding affinity between aptamers and their intended target, as this information determines how analytical assays based on aptamers are designed. Other analytical attributes that can be determined include: selectivity of aptamers for the target of interest over likely interferences; robustness of apparent affinity in complex matrices (such as full-strength or diluted biofluids); thermodynamic and kinetic binding parameters (ΔH, ΔS, ΔG, k_{on}, k_{off}); limit of detection; limit of quantitation; and sensitivity. If an aptamer is intended for use as the recognition element in an affinity assay, it may need first to be characterized in a wide range of conditions (pH, temperature, ionic strength, presence of particular cations) that may influence binding in the context of an assay. Finally, many aptamer researchers perform truncation studies to identify the smallest functional unit required for binding.[28–30] A simple version of a truncation study is to characterize the binding of both full-length aptamer—a random region plus primer-binding domains—and random region alone. Initially identified sequences may be varied *via* stochastic or rationally designed processes to converge on deeper minima in the binding energy landscape. The binding site can be identified through structural determination methods such as X-ray diffraction or systematic sequence alteration.[31] All such characterization experiments are costly in their consumption of aptamer and target, suggesting that efforts to miniaturize these assays would be of value.

[a]*Integrated Biomedical Sciences Graduate Program, University of Notre Dame, Notre Dame, IN, USA*

[b]*Department of Chemistry and Biochemistry, University of Notre Dame, Notre Dame, IN, USA. E-mail: rwhelan1@nd.edu*

† Electronic supplementary information (ESI) available: Fig. S1–S7 and Table S1. See DOI: 10.1039/d0ay02256j

Fluorescence anisotropy (FA; also known as fluorescence polarization, FP) assays have been used by researchers in the aptamer community to characterize aptamer–target binding since the early 1990s[16] and remain one of the most frequently used methods for this purpose.[32,33] FA assays use plane-polarized light to excite a fluorophore; the extent of depolarization of emitted fluorescence resulting from rotational diffusion is monitored. In the unbound state, fluorescently labelled aptamer undergoes rapid rotational diffusion and emits fluorescence that is depolarized (low anisotropy). Provided that the target is of sufficiently large molecular volume, aptamer–target binding forms a complex with slower rotational diffusion and emits fluorescence that is more polarized (high anisotropy). Typically, the concentration of a fluorescently labelled aptamer is held constant while concentration of target is systematically increased.[34] Plots of anisotropy change *vs.* target concentration can be fit with an appropriate binding model to extract parameters such as equilibrium binding affinity and stoichiometry.[32,35] Advantages of FA for aptamer characterization include compatibility with direct (rather than competitive) assays, avoiding the need for fluorescently labelled target, and the fact that detection occurs in free solution, without the need to separate bound aptamers from free.

In addition to their use in characterizing aptamers, FA assays support research in drug discovery.[36] Researchers from Amersham Biosciences UK reported an assay using 384- and 1536-well plates in which Cy-Dye labelled peptide and non-peptide ligands were used to probe two important G-protein-coupled receptors.[37] A miniaturized FA assay to screen small molecule libraries of potentially novel RNA–protein interactions has been reported.[38] In a displacement-based assay, Famulok and co-workers used fluorescently labelled guanosine exchange factor (GEF)-binding aptamers to screen for antagonists of the cytohesin class of GEFs.[39] In all these cases, miniaturization reduced the consumption of costly reagents without harming assay performance. Miniaturization of aptamer-based FA assays may benefit ongoing efforts to identify new drug targets and aptamer-based therapeutics.[40,41] A complementary application of miniaturized FA is for assays in which aptamers replace antibodies, such as in vaccine potency screening, as has been reported by researchers at Merck.[42]

Using high-efficiency (HE) 384-well plates, we find that the volume of a FA-aptamer assay can be reduced to 2 μL with minimal degradation of analytical performance compared to assays conducted in larger volumes. This small volume requirement enables improved efficiency over previously published work, in which assays were performed in quartz cuvettes in serial fashion[43–46] or in regular format 96- or 384-well plates.[47–49] Further, we report that the time of the assay—when using thrombin and two thrombin-binding aptamers[6,50] as a model system—can be easily be reduced from 60 minutes to 20 minutes from mixing to measuring, which also supports assay efficiency. Finally, for the thrombin-binding 29mer ssDNA aptamer and assay volumes ranging from 2 μL to 60 μL, binding data are well-modelled by the Hill equation with Hill coefficients > 1, indicating positive cooperativity. A single-site binding model fits the binding data less well, with higher percent relative standard error (%RSE) across all sample volumes and incubation times tested. In volumes larger than 10 μL, the Hill equation also better describes the binding of thrombin to the 15mer aptamer. Using the Hill equation to model binding in the thrombin–aptamer system is not standard practice, but it is suggested as correct by this work, as well as previous reports by us[48] and others.[49–54]

Experimental

Materials and reagents

Two thrombin-binding aptamers were obtained from Integrated DNA Technologies (Coralville, IA). The sequence of the 15mer was 5′-GGT TGG TGT GGT TGG-3′. The sequence of the 29mer was 5′-AGT CCG TGG TAG GGC AGG TTG GGG TGA CT-3′. Both aptamers were 5′ labelled with Texas Red, HPLC purified, and provided as the lyophilized solid. Aptamers were reconstituted to 100 μM in TE buffer (10 mM Tris, 0.1 mM EDTA, pH 8.0). TG buffer (192 mM Tris, 25 mM glycine) and KH_2PO_4 were purchased from VWR. TGK buffer was prepared by adding KH_2PO_4 to TG buffer to a final potassium ion concentration of 5 mM. Lyophilized thrombin from human plasma was purchased from Sigma and reconstituted to 1000 U mL^{-1} in a solution of 1 mg mL^{-1} bovine serum albumin (BSA) in MilliQ pure water. Low volume (≤20 μL) assays were performed in high efficiency 96- or 384-well black microplates (Molecular Devices). For volumes greater than 20 μL, flat-bottomed black 384-well plates from Greiner Bio-one were used.

Fluorescence anisotropy assays

Fluorescence anisotropy assays were performed with excitation at 585 nm, emission at 635 nm, and a cut-off at 610 nm in a SpectraMax M5 plate reader (Molecular Devices). 2.5 μM aptamer stock solutions were prepared in TE buffer. These aptamer solutions were diluted to 455 nM in TGK, heated to 95 °C for 3 minutes, and then cooled and held at 4 °C. Final sample solutions were prepared in TGK and contained 0.2 mg mL^{-1} BSA, 75 nM aptamer, and varied concentrations of thrombin (0–1070 nM).

Samples were loaded in triplicate for each different test volume into multi-well plates, with TGK as a reference blank. Each well was read 3 times for a total of 9 reads per sample. Volumes assayed were 2, 5, 10, 18, and 60 μL per well. Plates were covered with an optical adhesive cover (Applied Biosystems), incubated in the dark at 25 °C, and read after 20, 40, and 60 minutes. Prior to incubation, plates were spun at 50*g* for 2 minutes to ensure even coverage of the bottom of each well. Adhesive covers were removed before each measurement. The described method was repeated using the 29mer with 1 and 0.5 μL per well to establish the lower volume limit of the technique.

Data analysis

Binding data were fit with a Hill equation or with a single-site binding isotherm using non-linear least squares regression in *R* (nls function in the stats package of base *R*).[55] Curves were generated from mean values per sample. Standard error (SE)

and root-mean-squared error (RMSE) due to the regression were calculated by the nls function[55] for the constant values (K_A, K_d, and n). Briefly: SE is the standard deviation divided by the square root of n, and RMSE is the square root of the mean of the square of all the error (used as a parameter of goodness-of-fit). Percent relative standard error (%RSE) is calculated by dividing the standard error by the mean. Well-to-well variability was low, with all %RSE values of anisotropy among wells of the same volume and concentrations $\leq$ 5%.

Results and discussion

Decreasing volume and time in standard 384-well plates

Our research group routinely conducts FA assays to characterize binding between aptamers and protein targets.[48,56,57] In assays of this type, the target is typically expensive, available in limited amounts, or otherwise precious. The aptamer, meanwhile, is fluorescently labelled and purified by HPLC; both these modifications add to the aptamers' cost. Standard-format 96- and 384-well plates typically require the consumption of 10–100 μL of sample per well. Conducting an appropriately thorough characterization is therefore costly in time and resources. We were motivated to improve the efficiency of aptamer-based FA assays by reducing assay volume and decreasing the time from mixing to measurement. Beginning from a set of conditions that we have used successfully in 96- and 384-well flat-bottom plates (60 μL per well; 60 min incubation), we reduced the volume and the time between sample preparation and measurement in these plates, using thrombin and the thrombin-binding 29mer as a model system. Binding data were fit with the Hill equation (eqn (1)).

$$f_b = \frac{B_{max}[P]^n}{K_A{}^n + [P]^n} \quad (1)$$

For volumes of 60 μL per well and incubation times of 60, 40, and 20 min, calculated K_A values (in nM) were 45 ± 3, 46 ± 2, and 46 ± 2, respectively (Fig. S1†). When volume was reduced to 20 μL per well, with 60 min incubation, K_A was found to be 56 ± 4 nM (data not shown). From these data we conclude that the incubation time can be decreased to 20 min without change of apparent binding affinity in this model system. The reduction in volume in a standard format 384-well plate resulted in a value in reasonable agreement with higher volumes. Note that the Hill equation returns K_A as a metric of binding, and n, the Hill coefficient. K_A represents the concentration of protein at half-maximal binding, and n reports on cooperativity. When $n = 1$, the Hill equation collapses to the single-site binding square hyperbola, and $K_A = K_d$. Standard error for binding metric values were calculated by the nonlinear regression.

Decreasing incubation time in HE 96-well plates

We conducted binding assays using thrombin and the 29mer aptamer in high-efficiency 96-well plates, at a volume of 45 μL per well. For incubation times of 60, 40, and 20 min, calculated K_A values (in nM) were 49 ± 2, 45 ± 2, and 45 ± 2, respectively (Fig. S2†). The good agreement of these values indicates that the incubation time for this assay in HE 96-well plates can be decreased to 20 min without change to the determined affinity. We also observe that the conical shape of the wells in HE plates is compatible with aptamer FA assays.

Decreasing volume in HE 384-well plates

We sought to determine the smallest sample volume that could reliably characterize aptamer–target binding in HE 384-well plates. Using thrombin and the 29mer and 15mer aptamers in separate experiments, we collected binding isotherms in solutions ranging from a minimum of 2 μL to a maximum of 18 μL. All samples were incubated for 20 min before measurement. Representative overlaid binding isotherms are presented in Fig. 1 and 2 (for the 29mer and 15mer, respectively) and show that measured affinity is essentially indistinguishable over this volume range, suggesting that a 30-fold reduction in assay volume from our standard conditions is possible. The resulting data including additional evaluations of each volume at 40 and 60 min are also tabulated in Table 1 and reflect a modest decrease in assay precision at the lowest sample volumes as reflected in increased standard error. We find K_A values that are in good agreement with previous reports.[48] When the volume per well was decreased to 1 μL, the loss in precision was dramatic when compared to the other volumes assayed (Fig. S3†), indicating that the practical limit for these FA assays is 2 μL per well. 0.5 μL per well produced plots that did not resemble binding isotherms (data not shown).

Aptamer–thrombin binding is correctly modelled by the Hill equation with cooperativity > 1

The interaction of thrombin to its 15mer and 29mer aptamers is often fit using a simple 1 : 1 binding model. We and others have previously suggested that the interaction is more appropriately modelled using the Hill equation, which accounts for cooperative

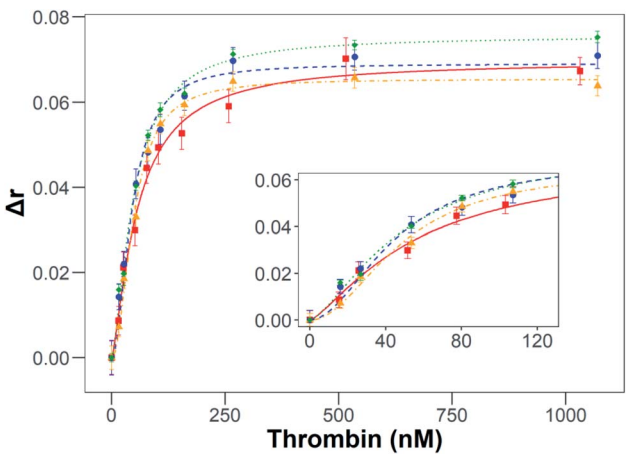

Fig. 1 29mer and thrombin binding curves after 20 minute incubation at varied volume per well in HE 384-well plates. 2 μL: red squares, solid; 5 μL: blue circles, dashed; 10 μL: yellow triangles, dot/dash; 18 μL: green diamond, dotted. Error bars are standard error of replicate measurements (n = 9). Each curve fit with the Hill equation. Inset shows low concentration range. Δr is change in anisotropy.

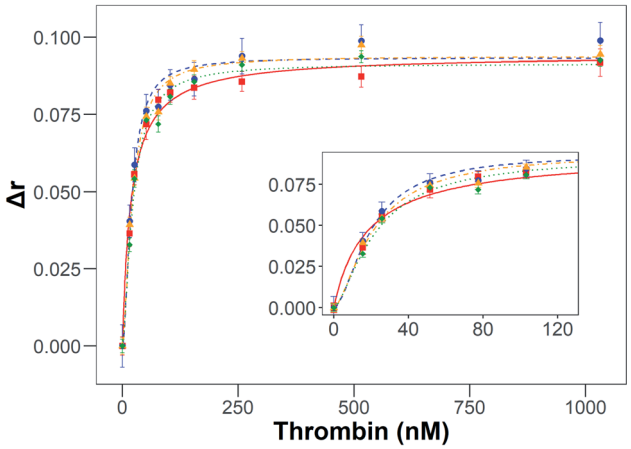

Fig. 2 15mer and thrombin binding curves after 20 minute incubation at varied volume per well in HE 384-well plates. 2 μL: red squares, solid; 5 μL: blue circles, dashed; 10 μL: yellow triangles, dot/dash; 18 μL: green diamond, dotted. Error bars are standard error of replicate measurements (n = 9). Each curve fit with the Hill equation. Inset shows low concentration range. Δr is change in anisotropy.

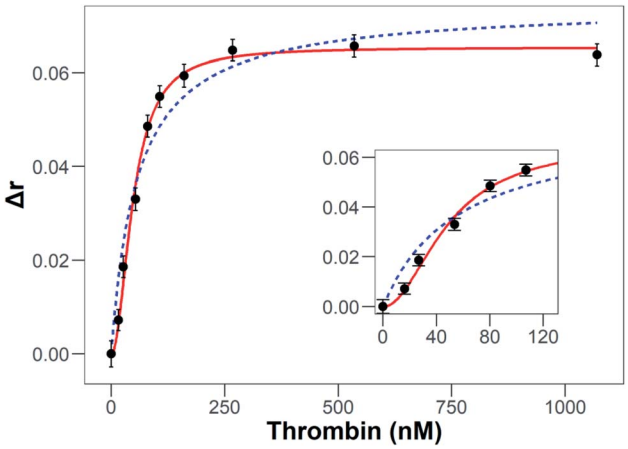

Fig. 3 29mer and thrombin binding curve, 10 μL per well, 20 minute incubation, fit with the Hill equation (red, solid) and Square Hyperbola Equation (blue, dashed). Assay performed in HE 384-well plate. Error bars are standard error of replicate measurements (n = 9). Inset shows low concentration range. Δr is change in anisotropy.

Table 1 Affinity of thrombin–aptamer binding determined from FA assays in various sample volumes and incubation times. Data were fit using eqn (1). All assays performed in HE 384 well plates. Standard error for the binding metric (K_A) was calculated from the nonlinear regression

Volume per well (μL)	Incubation time (minutes)	K_A (nM), 15mer	K_A (nM), 29mer
18	20	22 ± 2	48 ± 2
18	40	21 ± 1	46 ± 2
18	60	19 ± 1	47 ± 2
10	20	21 ± 1	48 ± 2
10	40	22 ± 1	51 ± 3
10	60	19 ± 2	49 ± 3
5	20	20 ± 2	45 ± 4
5	40	18 ± 1	46 ± 3
5	60	15 ± 1	45 ± 3
2	20	19 ± 2	56 ± 5
2	40	17 ± 2	61 ± 7
2	60	16 ± 2	63 ± 6

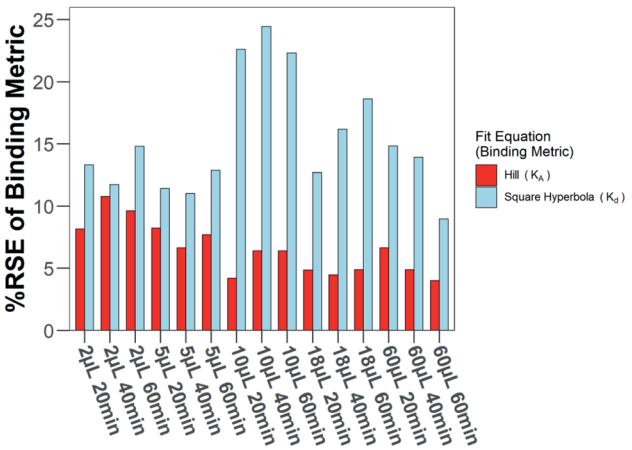

Fig. 4 29mer aptamer and thrombin binding assays. Comparison of fit quality for Hill equation and Square Hyperbola Equation by percent relative standard error (%RSE) values of K_A and K_d respectively. Hill equation fit (K_A) – red; Square Hyperbola Equation fit (K_d) – light blue. %RSE calculated during nonlinear regression. Labels are volume per well and incubation time. For volumes less than 20 μL, assays performed in HE 384 well plates. For volumes greater than 20 μL, assays performed in normal 384 well plates.

binding.[48–54] As stated earlier, cooperative binding is indicated by values of the Hill coefficient (n) > 1 (see Table S1† for calculated n values). Binding curves collected on small volumes in high-efficiency plates display positive cooperativity. Evidence substantiating this claim is found in Fig. 3 and 4. Fig. 3 shows a representative thrombin and 29mer binding curve, fit with both the square hyperbola equation (blue, dashed) and the Hill equation (red, solid). Visual inspection suggests that the Hill equation is the better fit. Fig. S4† shows the same plot for the 15mer.

Quantitative comparison of the two binding models is shown in Fig. 4, in which percent relative standard error (%RSE) for the values of K_A (from the Hill equation) and K_d (from the square hyperbola) are shown. The Hill equation provides a better fit to the measured binding data. A similar trend is observed for the 15mer aptamer in volumes greater than 10 μL (Fig. S5†) and when root-mean-squared error (RMSE) is used as the metric of binding quality (Fig. S6 and S7†). We have previously noted that the cooperative binding of the 15mer is less obvious than that of the 29mer.[48] At volumes ≤ 10 μL we hypothesize that the slight loss in precision due to lower volumes means that the model is no longer able to differentiate cooperative from non-cooperative binding in the 15mer system.

Conclusions

The low-volume FA aptamer assay demonstrated here may find many useful applications. It will expand the ability of aptamer

researchers to screen more aptamer candidates at the conclusion of a SELEX experiment, leading to higher success rates of selection processes. Although the assays reported here were performed manually, they could readily be automated with a liquid-handling robot, enabling rapid screening of many aptamer candidates and modified (*e.g.* truncated) variants. Binding in diverse sample matrices (*e.g.* biofluids) could be screened in an automated fashion. Function, such as therapeutic activity, could be screened with greater efficiency, saving time and resources. Efforts to automate this assay in 384- and 1536-well plates are ongoing. Furthermore, the assay as demonstrated here requires minimal expertise and can be immediately used by others in academic or industrial research settings. Finally, we emphasize the importance of correctly modelling aptamer–target binding data. The simplest binding model (1 : 1 stoichiometry) is not appropriate for all aptamer–target systems, including the widely used thrombin model system.

Author contributions

Simon D. Weaver: Investigation, writing, reviewing, and editing. Rebecca J. Whelan: Conceptualization, writing, reviewing, and editing.

Conflicts of interest

There are no conflicts to declare.

Acknowledgements

This work was supported by the University of Notre Dame Advancing Our Vision Fund in Analytical Science and Engineering (to RJW). The authors thank Naviya Schuster-Little for her assistance with preparing the graphical abstract and the NSF Center for Bioanalytic Metrology for valuable discussions.

References

1 M. R. Dunn, R. M. Jimenez and J. C. Chaput, *Nat. Rev. Chem.*, 2017, **1**, 1–16.
2 T. Wang, C. Chen, L. M. Larcher, R. A. Barrero and R. N. Veedu, *Biotechnol. Adv.*, 2019, **37**, 28–50.
3 W. Xu, W. He, Z. Du, L. Zhu, K. Huang, Y. Lu and Y. Luo, *Angew. Chem., Int. Ed.*, 2020, **59**, 2–31.
4 A. D. Ellington and J. W. Szostak, *Nature*, 1990, **346**, 818–822.
5 C. Tuerk and L. Gold, *Science*, 1990, **249**, 505–510.
6 L. C. Bock, L. C. Griffin, J. A. Latham, E. H. Vermaas and J. J. Toole, *Nature*, 1992, **355**, 564–566.
7 D. E. Volk and G. L. R. Lokesh, *Biomedicines*, 2017, **5**, 41.
8 J. P. Elskens, J. M. Elskens and A. Madder, *Int. J. Mol. Sci.*, 2020, **21**, 4522.
9 R. D. Jenison, S. C. Gill, A. Pardi and B. Polisky, *Science*, 1994, **263**, 1425–1429.
10 D. E. Huizenga and J. W. Szostak, *Biochemistry*, 1995, **34**, 656–665.
11 D. Jellinek, L. S. Green, C. Bell and N. Janjic, *Biochemistry*, 1994, **33**, 10450–10456.
12 T. W. Wiegand, P. B. Williams, S. C. Dreskin, M.-H. Jouvin, J.-P. Kinet and D. Tasset, *J. Immunol.*, 1996, **157**, 221–230.
13 K. N. Morris, K. B. Jensen, C. M. Julin, M. Weil and L. Gold, *Proc. Natl. Acad. Sci. U. S. A.*, 1998, **95**, 2902–2907.
14 B. J. Hicke, C. Marion, Y.-F. Chang, T. Gould, C. K. Lynott, D. Parma, P. G. Schmidt and S. Warren, *J. Biol. Chem.*, 2001, **276**, 48644–48654.
15 C. L. A. Hamula, H. Zhang, L. L. Guan, X.-F. Li and X. C. Le, *Anal. Chem.*, 2008, **80**, 7812–7819.
16 L. B. McGown, M. J. Joseph, J. B. Pitner, G. P. Vonk and C. P. Linn, *Anal. Chem.*, 1995, 663A–668A.
17 I. German, D. D. Buchanan and R. T. Kennedy, *Anal. Chem.*, 1998, **70**, 4540–4545.
18 J. R. Cole, L. W. Dick Jr, E. J. Morgan and L. B. McGown, *Anal. Chem.*, 2007, **79**, 273–279.
19 R. A. Potyrailo, R. C. Conrad, A. D. Ellington and G. M. Hieftje, *Anal. Chem.*, 1998, **70**, 3419–3425.
20 T. G. McCauley, N. Hamaguchi and M. Stanton, *Anal. Biochem.*, 2003, **319**, 244–250.
21 L. Wang, X. Liu, X. Hu, S. Song and C. Fan, *Chem. Commun.*, 2006, 3780–3782.
22 P. Liang, J. Canoura, H. Yu, O. Alkhamis and Y. Xiao, *ACS Appl. Mater. Interfaces*, 2018, **10**, 4233–4242.
23 B. R. Baker, R. Y. Lai, M. S. Wood, E. H. Doctor, A. J. Heeger and K. W. Plaxco, *J. Am. Chem. Soc.*, 2006, **128**, 3138–3139.
24 A. Shaver, S. D. Curtis and N. Arroyo-Currás, *ACS Appl. Mater. Interfaces*, 2020, **12**, 11214–11223.
25 Y. Wu, I. Belmonte, K. S. Sykes, Y. Xiao and R. J. White, *Anal. Chem.*, 2019, **91**, 15335–15344.
26 M. Berezovski, M. Musheev, A. Drabovich and S. N. Krylov, *J. Am. Chem. Soc.*, 2006, **128**, 1410–1411.
27 J. Wang, J. Yu, Q. Yang, J. McDermott, A. Scott, M. Vukovich, R. Lagrois, Q. Gong, W. Greenleaf, M. Eisenstein, B. S. Ferguson and H. T. Soh, *Angew. Chem., Int. Ed.*, 2017, **56**, 744–747.
28 J. Akitomi, S. Kato, Y. Yoshida, K. Horii, M. Furuichi and I. Waga, *Bioinformation*, 2011, **6**, 38–40.
29 W. M. Rockey, F. J. Hernandez, S.-Y. Huang, S. Cao, C. A. Howell, G. S. Thomas, X. Y. Liu, N. Lapteva, D. M. Spencer, J. O. McNamara, X. Zou, S.-J. Chen and P. H. Giangrande, *Nucleic Acid Ther.*, 2011, **21**, 299–314.
30 T. T. Le, O. Chumphukam and A. E. G. Cass, *RSC Adv.*, 2014, **4**, 47227–47233.
31 D. Zhang, M. Lu and H. Wang, *J. Am. Chem. Soc.*, 2011, **133**, 9188–9191.
32 M. Jing and M. T. Bowser, *Anal. Chim. Acta*, 2011, **686**, 9–18.
33 Q. Zhao, J. Tao, W. Feng, J. S. Uppal, H. Peng and X. C. Le, *Anal. Chim. Acta*, 2020, **1125**, 267–278.
34 G. Gokulrangan, J. R. Unruh, D. F. Holub, B. Ingram, C. K. Johnson and G. S. Wilson, *Anal. Chem.*, 2005, **77**, 1963–1970.
35 R. Thevendran, T. N. Navien, X. Meng, K. Wen, Q. Lin, S. Sarah, T.-H. Tang and M. Citartan, *Anal. Biochem.*, 2020, **600**, 113742.

36 A. Uri and O. E. Nonga, *Expert Opin. Drug Discovery*, 2020, **15**, 131–133.
37 A. Harris, S. Cox, D. Burns and C. Norey, *J. Biomol. Screening*, 2003, **8**, 410–420.
38 C. Mao, K. G. Flavin, S. Wang, R. Dodson, J. Ross and D. J. Shapiro, *Anal. Biochem.*, 2006, **350**, 222–232.
39 M. Hafner, E. Vianini, B. Albertoni, L. Marchetti, C. Gloeckner and M. Famulok, *Nat. Protoc.*, 2008, **3**, 579–587.
40 J. Zhou and J. Rossi, *Nat. Rev. Drug Discovery*, 2017, **16**, 181–202.
41 S. M. Nimjee and B. A. Sullenger, *Curr. Med. Chem.*, 2020, **27**, 4181–4193.
42 J. J. Trausch, M. Shank-Retzlaff and T. Verch, *Vaccine*, 2017, **35**, 5495–5502.
43 X. Cai, S. Xu, Z. Zhang, Z. Liu and W. Lu, *Proc. SPIE*, 2001, **4414**, 50–52.
44 X. Fang, Z. Cao, T. Beck and W. Tan, *Anal. Chem.*, 2001, **73**, 5752–5757.
45 W. Li, K. Wang, W. Tan, C. Ma and X. Yang, *Analyst*, 2007, **132**, 107–113.
46 Y. Liu and Q. Zhao, *Anal. Methods*, 2016, **8**, 2383.
47 Z. Zhu, C. Ravelet, S. Perrier, V. Guieu, E. Fiore and E. Peyrin, *Anal. Chem.*, 2012, **84**, 7203–7211.
48 K. S. Mears, D. L. Markus, O. Ogunjimi and R. J. Whelan, *Aptamers*, 2018, **2**, 64–73.
49 A. V. Samokhvalov, I. V. Safenkova, S. A. Eremin, A. V. Zherdev and B. D. Dzantiev, *Anal. Chem.*, 2018, **90**, 9189–9198.
50 D. M. Tasset, M. F. Kubuk and W. Steiner, *J. Mol. Biol.*, 1997, **272**, 688–698.
51 K. Padmanabhan, K. P. Padmanabhan, J. D. Ferrara, J. E. Sadler and A. Tulinsky, *J. Biol. Chem.*, 1993, **268**, 17651–17654.
52 K. Padmanabhan and A. Tulinksy, *Acta Crystallogr., Sect. D: Biol. Crystallogr.*, 1996, **52**, 272–282.
53 B. Pagano, L. Martino, A. Randazzao and C. Giancola, *Biophys. J.*, 2008, **94**, 562–569.
54 P. Baaske, C. J. Wienken, P. Reineck, S. Duhr and D. Braun, *Angew. Chem., Int. Ed.*, 2010, **49**, 2238–2241.
55 R Core Team, *R: A language and environment for statistical computing*, (v. 4.0.2), R Foundation for Statistical Computing, Vienna, Austria, 2020.
56 R. M. Eaton, J. A. Shallcross, L. E. Mael, K. S. Mears, L. Minkoff, D. J. Scoville and R. J. Whelan, *Anal. Bioanal. Chem.*, 2015, **407**, 6965–6973.
57 D. J. Scoville, T. K. B. Uhm, J. A. Shallcross and R. J. Whelan, *J. Nucleic Acids*, 2017, **2017**, 9879135.